Synthesis of Ethylene Tethered Isatin-Coumarin Hybrids and Evaluation of Their *in vitro* Antimycobacterial Activities

Tao Gao,[a,b*†] Zhigang Zeng,[b†] Gangqiang Wang,[b] Shaofa Sun,[b*] and Yi Liu[a*]

[a]State Key Laboratory of Virology & Key Laboratory of Analytical Chemistry for Biology and Medicine (Ministry of Education), College of Chemistry and Molecular Sciences, Wuhan University, Wuhan 430072, People's Republic of China
[b]School of Nuclear Technology and Chemistry & Biology, Hubei University of Science and Technology, Xianning 437100, People's Republic of China
*E-mail: gaotao@whu.edu.cn; sunshaofa@hbust.edu.cn; yiliuchem@whu.edu.cn
†These authors contributed equally.

Received January 9, 2018
DOI 10.1002/jhet.3161
Published online 00 Month 2018 in Wiley Online Library (wileyonlinelibrary.com).

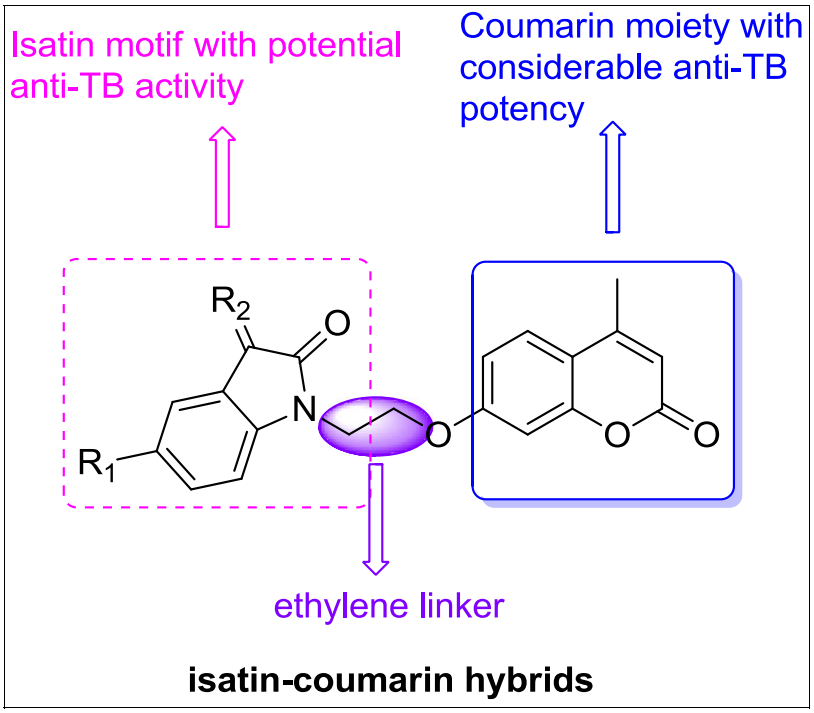

A series of novel isatin-coumarin derivatives tethered through ethylene were designed, synthesized, and evaluated for their in vitro antimycobacterial activities against Mycobacterium tuberculosis (MTB) H37Rv and multidrug-resistant tuberculosis (MDR-TB). All hybrids exhibited potential antimycobacterial activities against MTB H37Rv and MDR-TB with minimum inhibitory concentration (MIC) ranging from 32 to 256 μg/mL. In particular, the hybrid **4h** (MIC: 50 and 32 μg/mL) was most active against MTB H_{37}Rv and MDR-TB strains, which was 2 and >4 folds more potent than the first-line antitubercular agents rifampicin (MIC: 64 μg/mL) and isoniazid (MIC: >128 μg/mL) against MDR-TB, warrant further optimization.

INTRODUCTION

Tuberculosis (TB), which is caused predominately by *Mycobacterium tuberculosis* (MTB), is the ninth leading cause of death globally and the leading cause from a single infectious agent, ranking above HIV/AIDS [1]. According to the World Health Organization latest estimation, around 10.4 million newly TB cases with 1.67 million deaths occurred in the year 2016 and 1.7 billion people infected with MTB will develop TB disease during their lifetime [1]. TB is the most common opportunistic infection affecting HIV-positive individuals, resulted in 374,000 deaths in 2016. Interactions between HIV and TB medications and immune reconstitution inflammatory syndrome making treatment of TB in HIV-infected individuals are of great challenge [2,3]. Moreover, the incidence of drug-resistant TB (DR-TB) such as multidrug-resistant TB (MDR-TB) making the first-line anti-TB agents such as isoniazid (INH), rifampicin (RIF), pyrazinamide (PZA), and ethambutol (EMB) more and more ineffective, which has further aggravated the mortality and spread of

this disease [4,5]. Thus, it is imperative to develop new anti-TB agents without drug interaction with anti-HIV medications, and with new action mechanism to overcome the resistance.

Isatin and coumarin act as structural subunits of more complex natural products, occupy a pivotal position in medicinal chemistry. Their derivatives exhibited diverse biological properties such as antibacterial [6,7], anticancer [8], antimalarial [9], antifungal [10], and anti-TB profiles [11–15]. Furthermore, several isatin or coumarin based drugs such as sunitinib, nintedanib, warfarin, and hymecromone have been approved for clinical use for the treatment of various diseases [16]. Thus, hybridization of isatin and coumarin into one molecule may provide potential anti-TB candidates.

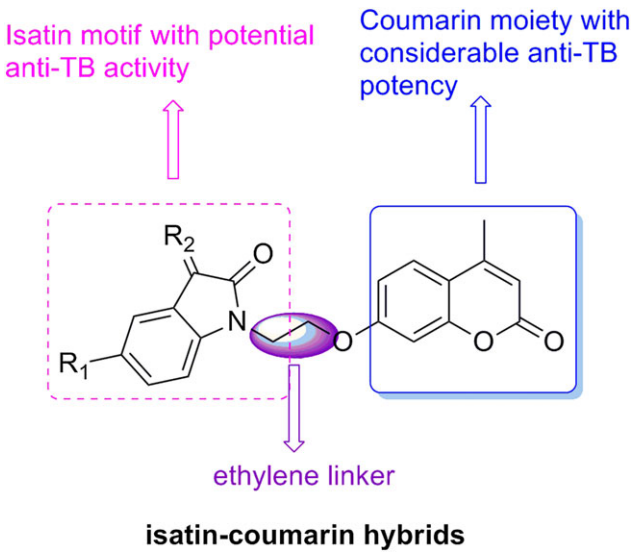

Figure 1. Illustration of design strategy. [Color figure can be viewed at wileyonlinelibrary.com]

Recently, several isatin-coumarin hybrids tethered through 1,2,3-triazolyl were screened for their antimycobacterial activities by different groups, and some of showed potential potency [14,16]. Based on the aforementioned research results and as a continuous research program to optimize the linker between isatin and coumarin, a set of novel isatin-coumarin hybrids tethered through ethylene was designed, synthesized, and assessed for their in vitro antimycobacterial activities against MTB H37Rv and MDR-TB in this study. Illustration of the design strategy for ethylene tethered isatin-coumarin hybrids is depicted in Figure 1.

RESULTS AND DISCUSSION

The synthetic pathway for propylene-tethered isatin-coumarin hybrids **5a**–**j** was depicted in Scheme 1. Isatin and 5-fluoroisatin was alkylated with 1,2-dibromoethane in the presence of potassium carbonate to provide the corresponding *N*-(2-bromoethyl)isatin and *N*-(2-bromoethyl)-5-fluoroisatin **2** (yield: 49% and 57%) by literature methods [17,18]. The targets **5a**,**b** were obtained by reacting intermediates **2** with 7-hydroxy-4-

Scheme 1. Synthesis of ethylene tethered isatin-coumarin hybrids **5a**–**j**.

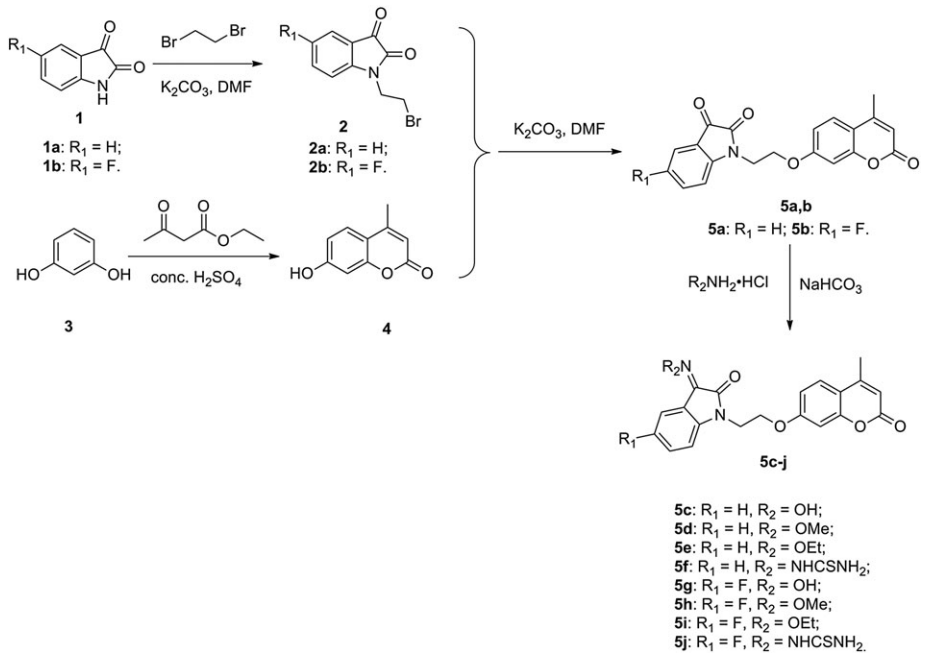

methyl-7-2*H*-chromen-2-one **4** in presence of potassium carbonate [19]. Finally, condensations of targets **5a**,**b** with hydroxylamine or methoxyamine or ethoxyamine hydrochloride in the presence of sodium bicarbonate provided targets **5c**–**j** (28–57%) [20].

All ethylene tethered isatin-coumarin hybrids **5a**–**j** were evaluated for their in vitro antimycobacterial activities against MTB $H_{37}Rv$ and MDR-TB strains (see Table 1). The MDR-TB strain was resistant to INH, RIF, and EMB. The minimum inhibitory concentration (MIC) is defined as the lowest concentration that inhibits the visible bacterial growth.

The results showed that all ethylene tethered isatin-coumarin hybrids **5a**–**j** displayed potential antimycobacterial activities against MTB $H_{37}Rv$ and MDR-TB strains with MIC ranging from 32 to 256 μg/mL. The structure–activity relationship indicated that 5-fluoroisatin hybrids **5f**–**j** were more potent than the corresponding unsubstituted **5a**–**e**: substituents at C-3 position of isatin moitif have great influence on the activity, and the relative contribution of the substituents to the activity was as follows: NOMe > $NNHCSNH_2$ > O > NOEt > NOH.

It is worth to notice that the resistance index for almost all ethylene tethered isatin-coumarin hybrids was around 1, and four of them was <1, indicating they may have novel action mechanism.

Among them, the conjugate **5h** (MIC: 50 and 32 μg/mL) was most active against MTB $H_{37}Rv$ and MDR-TB strains, which was 2 and >4 folds more potent than the first-line anti-TB agents RIF (MIC: 64 μg/mL) and INH (MIC: >128 μg/mL) against MDR-TB, warrant further investigations.

Table 1

Structures and antimycobacterial activities of hybrids **5a**–**j**.

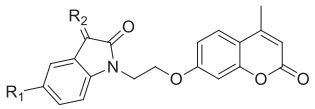

Compd.	R_1	R_2	MIC (μg/mL) MTB $H_{37}Rv$	MDR-TB
5a	H	O	100	128
5b	H	NOH	200	256
5c	H	NOMe	100	32
5d	H	NOEt	100	256
5e	H	$NNHCSNH_2$	100	64
5f	F	O	100	64
5g	F	NOH	200	256
5h	F	NOMe	50	32
5i	F	NOEt	100	128
5j	F	$NNHCSNH_2$	50	64
INH	—	—	0.05	>128
RIF	—	—	0.39	64

MIC, minimum inhibitory concentration; MTB, Mycobacterium tuberculosis; MDR-TB, multidrug-resistant tuberculosis; INH, isoniazid; RIF, rifampicin.

CONCLUSION

In summary, a new class of novel ethylene tethered isatin-coumarin hybrids was designed, synthesized, and evaluated for their in vitro antimycobacterial activities against MTB H37Rv and MDR-TB in this paper. All hybrids exhibited considerable activities against the tested strains, the enriched structure–activity relationship paves the way for further optimization of this kind of hybrids.

EXPERIMENTAL SECTION

Synthesis. General procedure for the preparation of targets 5a,**b**. *N*-(3-bromopropyl)isatins **2a**,**b** were obtained according to the literature reported method [17,18]. A mixture of *N*-(3-bromopropyl)isatins **2a**,**b** (5 mmol), 7-hydroxy-4-methyl-7-2*H*-chromen-2-one **4** (3 mmol), and K_2CO_3 (20 mmol) was stirred at room temperature for 2 days. After filtration, the filtrate was concentrated in vacuo. The residue was purified by silica gel chromatography eluted with PE:EA = 1:1 to give **5a**, **b** as light yellow solids.

1-(2-((4-Methyl-2-oxo-2H-chromen-7-yl)oxy)ethyl)indoline-2,3-dione (5a). Yellow solid. ^{1}H NMR (400 MHz, DMSO-d_6) δ 2.36 (3H, s, Me), 4.12 (2H, t, ─CH_2─), 4.34 (2H, t, ─CH_2─), 6.21 (1H, s, Ar─H), 6.88 (1H, dd, Ar─H), 6.90 (1H, d, Ar─H), 7.16 (1H, t, Ar─H), 7.34 (1H, d, Ar─H), 7.55 (1H, d, Ar─H), 7.71 (1H, d, Ar─H). ESI-MS *m*/*z*: 350 $[M + H]^+$. Elemental *Anal*. Calcd (%) for $C_{20}H_{15}NO_5$: C, 68.76; H, 4.33; N, 4.01; Found: C, 68.59; H, 4.17; N, 3.83.

5-Fluoro-1-(2-((4-methyl-2-oxo-2H-chromen-7-yl)oxy)ethyl) indoline-2,3-dione (5b). Yellow solid. ^{1}H NMR (400 MHz, DMSO-d_6) δ 2.34 (3H, s, Me), 4.12 (2H, t, ─CH_2─), 4.36 (2H, t, ─CH_2─), 6.21 (1H, s, Ar─H), 6.90 (1H, dd, Ar─H), 6.96 (1H, d, Ar─H), 7.38 (1H, dd, Ar─H), 7.46 (1H, dd, Ar─H), 7.59 (1H, dt, Ar─H), 7.67 (1H, d, Ar─H). ESI-MS *m*/*z*: 368 $[M + H]^+$. Elemental *Anal*. Calcd (%) for $C_{20}H_{14}FNO_5$: C, 65.40; H, 3.84; N, 3.81; Found: C, 65.19; H, 3.77; N, 3.65.

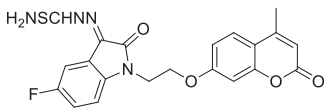

2-(5-fluoro-1-(2-((4-methyl-2-oxo-2*H*-chromen-7-yl)oxy)ethyl)-2-oxoindolin-3-ylidene)hydrazinecarbothioamide

The general procedure for preparing targets 5c–j. To a solution of substituted amine hydrochlorides (15 mmol) and $NaHCO_3$ (15 mmol) dissolved in water (10 mL) and methanol (50 mL) was added **5a**,**b** (5 mmol). The reaction mixture was stirred at room temperature for 24 h. After removal of the solvent, the residue was diluted with water (20 mL) and then filtered. The solid crude product was purified by column chromatography (silica gel) eluted with DCM to PE:EA = 1:1 to give the title targets **5c**–**j**.

3-(Hydroxyimino)-1-(2-((4-methyl-2-oxo-2H-chromen-7-yl) oxy)ethyl)indolin-2-one (5c). Yellow solid. ^{1}H NMR (400 MHz, DMSO-d_6) δ 2.35 (3H, s, Me), 4.13 (2H, t, ─CH_2─), 4.32 (2H, t, ─CH_2─), 6.21 (1H, s, Ar─H), 6.87 (1H, dd, Ar─H), 6.91 (1H, d, Ar─H), 7.15 (1H, t, Ar─H), 7.32 (1H, d, Ar─H), 7.51 (1H, d, Ar─H), 7.74 (1H, d, Ar─H), 13.40 (1H, brs, NOH). ESI-MS *m*/*z*: 365 $[M + H]^+$. Elemental *Anal*. Calcd (%) for $C_{20}H_{16}N_2O_5$: C, 65.93; H, 4.43; N, 7.69; Found: C, 65.82; H, 4.27; N, 7.46.

5-Fluoro-3-(hydroxyimino)-1-(2-((4-methyl-2-oxo-2H-chromen-7-yl)oxy)ethyl)indolin-2-one (5d). Yellow solid. ^{1}H NMR (400 MHz, DMSO-d_6) δ 2.34 (3H, s, Me), 4.12 (2H, t, ─CH_2─), 4.34 (2H, t, ─CH_2─), 6.21 (1H, s, Ar─H), 6.92 (1H, dd, Ar─H), 6.98 (1H, d, Ar─H), 7.37 (1H, dd, Ar─H), 7.46 (1H, dd, Ar─H), 7.61 (1H, dt, Ar─H), 7.68 (1H, d, Ar─H), 13.36 (1H, brs, NOH). ESI-MS *m*/*z*: 383 $[M + H]^+$. Elemental *Anal*. Calcd (%) for $C_{20}H_{15}F_2NO_5$: C, 62.83; H, 3.95; N, 7.33; Found: C, 62.71; H, 3.74; N, 7.21.

3-(Methoxyimino)-1-(2-((4-methyl-2-oxo-2H-chromen-7-yl) oxy)ethyl)indolin-2-one (5e). Yellow solid. ^{1}H NMR (400 MHz, DMSO-d_6) δ 2.31 (3H, s, Me), 4.12 (2H, t, ─CH_2─), 4.21 (3H, s, NOMe), 4.33 (2H, t, ─CH_2─), 6.21 (1H, s, Ar─H), 6.86 (1H, dd, Ar─H), 6.90 (1H, d, Ar─H), 7.18 (1H, t, Ar─H), 7.30 (1H, d, Ar─H), 7.52 (1H, d, Ar─H), 7.76 (1H, d, Ar─H). ESI-MS *m*/*z*: 379 $[M + H]^+$. Elemental *Anal*. Calcd (%) for $C_{21}H_{18}N_2O_5$: C, 66.66; H, 4.79; N, 7.40; Found: C, 66.52; H, 4.57; N, 7.23.

5-Fluoro-3-(methoxyimino)-1-(2-((4-methyl-2-oxo-2H-chromen-7-yl)oxy)ethyl)indolin-2-one (5f). Yellow solid. ^{1}H NMR (400 MHz, DMSO-d_6) δ 2.36 (3H, s, Me), 4.12 (2H, t, ─CH_2─), 4.21 (3H, s, NOMe), 4.34 (2H, t, ─CH_2─), 6.21 (1H, s, Ar─H), 6.94 (1H, dd, Ar─H), 6.98 (1H, d, Ar─H), 7.38 (1H, dd, Ar─H), 7.48 (1H, dd, Ar─H), 7.61 (1H, dt, Ar─H), 7.72 (1H, d, Ar─H). ESI-MS *m*/*z*: 397 $[M + H]^+$. Elemental *Anal*. Calcd (%) for $C_{21}H_{17}FN_2O_5$: C, 63.63; H, 4.32; N, 7.07; Found: C, 63.50; H, 4.14; N, 7.01.

3-(Ethoxyimino)-1-(2-((4-methyl-2-oxo-2H-chromen-7-yl) oxy)ethyl)indolin-2-one (5g). Yellow solid. ^{1}H NMR (400 MHz, DMSO-d_6) δ 1.34 (3H, t, $NOCH_2\underline{CH_3}$), 2.35 (3H, s, Me), 4.12 (2H, t, ─CH_2─), 4.32 (2H, t, ─CH_2─), 4.41 (2H, q, $NO\underline{CH_2}CH_3$), 6.21 (1H, s, Ar─H), 6.84 (1H, dd, Ar─H), 6.90 (1H, d, Ar─H), 7.16 (1H, t, Ar─H), 7.27 (1H, d, Ar─H), 7.51 (1H, d, Ar─H), 7.76 (1H, d, Ar─H). ESI-MS *m*/*z*: 393 $[M + H]^+$. Elemental *Anal*. Calcd (%) for $C_{22}H_{20}N_2O_5$: C, 67.34; H, 5.14; N, 7.14; Found: C, 67.21; H, 5.01; N, 7.03.

3-(Ethoxyimino)-5-fluoro-1-(2-((4-methyl-2-oxo-2H-chromen-7-yl)oxy)ethyl)indolin-2-one (5h). Yellow solid. ^{1}H NMR (400 MHz, DMSO-d_6) δ 1.35 (3H, t, $NOCH_2\underline{CH_3}$), 2.36 (3H, s, Me), 4.12 (2H, t, ─CH_2─), 4.32 (2H, t, ─CH_2─), 4.42 (2H, q, $NO\underline{CH_2}CH_3$), 6.21 (1H, s, Ar─H), 6.96 (1H, dd, Ar─H), 6.99 (1H, d, Ar─H), 7.35 (1H, dd, Ar─H), 7.47 (1H, dd, Ar─H), 7.63 (1H, dt, Ar─H), 7.74 (1H, d, Ar─H). ESI-MS *m*/*z*: 411 $[M + H]^+$. Elemental *Anal*. Calcd (%) for $C_{22}H_{19}FN_2O_5$: C, 64.39; H, 4.67; N, 6.83; Found: C, 64.19; H, 4.52; N, 6.61.

2-(1-(2-((4-Methyl-2-oxo-2H-chromen-7-yl)oxy)ethyl)-2-oxoindolin-3-ylidene)hydrazinecarbothioamide (5i). Yellow solid. ^{1}H NMR (400 MHz, DMSO-d_6) δ 2.36 (3H, s, Me), 4.12 (2H, t, ─CH_2─), 4.34 (2H, t, ─CH_2─), 6.22 (1H, s, Ar─H), 6.80 (1H, dd, Ar─H), 6.88 (1H, d, Ar─H), 7.14 (1H, t, Ar─H), 7.25 (1H, d, Ar─H), 7.52 (1H, d, Ar─H), 7.74 (1H, d, Ar─H), 8.76, 9.08 (1H, s, $NNHCS\underline{NH_2}$), 12.18 (1H, s, $N\underline{NH}CSNH_2$). ESI-MS *m*/*z*: 423 $[M + H]^+$. Elemental *Anal*. Calcd (%) for $C_{21}H_{18}N_4O_4S$: C, 59.70; H, 4.29; N, 13.26; Found: C, 59.59; H, 4.07; N, 13.11.

2-(5-Fluoro-1-(2-((4-methyl-2-oxo-2H-chromen-7-yl)oxy) ethyl)-2-oxoindolin-3-ylidene)hydrazinecarbothioamide (5j). Yellow solid. ^{1}H NMR (400 MHz, DMSO-d_6) δ 2.36 (3H, s, Me), 4.13 (2H, t, ─CH_2─), 4.32 (2H, t, ─CH_2─), 6.21 (1H, s, Ar─H), 6.97 (1H, dd, Ar─H), 7.01 (1H, d, Ar─H), 7.36 (1H, dd, Ar─H), 7.45 (1H, dd, Ar─H), 7.66 (1H, dt, Ar─H), 7.76 (1H, d, Ar─H), 8.78, 9.10 (1H, s, $NNHCS\underline{NH_2}$), 12.16 (1H, s, $N\underline{NH}CSNH_2$). ESI-MS *m*/*z*: 441 $[M + H]^+$. Elemental *Anal*. Calcd (%) for $C_{21}H_{17}FN_4O_4S$: C, 57.27; H, 3.89; N, 12.72; Found: C, 57.07; H, 3.71; N, 12.53.

MIC determination. Hybrids **5a**–**j** together with RIF and INH were evaluated for their in vitro activities against MTB H37Rv and MDR-TB via rapid direct susceptibility test technique [19]. The wells of a sterile 48-well plate were filled with 100 mL twofold diluted tested compounds and 100 mL MTB H37Rv or MDR-TB suspension containing 4 × 10–3 mg cells. Pure medium replaced the diluted compounds in two wells as the positive control of growth, and deionized water instead of the culture in other two wells as the negative control of growth in the plates. The plates were covered and sealed, then incubated at 37°C in a wet box. The positive and negative control wells should show obvious difference after 3 days. The MIC was determined by observing the quantity and state of the cells in each test well by a continuous visual high magnification system, and redetermined 7 days later. The MIC is defined as the concentration of the compound required to give complete inhibition of bacterial growth.

REFERENCES AND NOTES

[1] World Health Organization, Global Tuberculosis Report 2017.

[2] Hu, Y. Q.; Zhang, S.; Zhao, F.; Gao, C.; Feng, L. S.; Lv, Z. S.; Xu, Z.; Wu, X. Eur J Med Chem 2017, 133, 255.

[3] Hu, Y. Q.; Xu, Z.; Zhang, S.; Wu, X.; Ding, J. W.; Lv, Z. S.; Feng, L. S. Eur J Med Chem 2017, 136, 122.

[4] Zhang, S.; Xu, Z.; Gao, C.; Ren, Q. C.; Le, C.; Lv, Z. S.; Feng, L. S. Eur J Med Chem 2017, 138, 501.

[5] Xu, Z.; Gao, C.; Ren, Q. C.; Song, X. F.; Feng, L. S.; Lv, Z. S. Eur J Med Chem 2017, 139, 429.

[6] Hu, Y. Q.; Zhang, S.; Xu, Z.; Lv, Z. S.; Liu, M. L.; Feng, L. S. Eur J Med Chem 2017, 141, 335.

[7] Zhang, G. F.; Zhang, S.; Pan, B. F.; Liu, M. L.; Feng, L. S. Eur J Med Chem 2018, 143, 710.

[8] Gabr, M. T.; El-Gohary, N. S.; Elbendary, E. R.; El-Kerdawy, M. M.; Ni, N. Eur J Med Chem 2017, 128, 36.

[9] Hu, Y. Q.; Gao, C.; Zhang, S.; Xu, L.; Xu, Z.; Feng, L. S.; Wu, X.; Zhao, F. Eur J Med Chem 2017, 139, 22.

[10] Hu, X. L.; Xu, Z.; Liu, M. L.; Feng, L. S.; Zhang, G. D. Curr Top Med Chem 2018, 18. https://doi.org/10.2174/1568026618666171215100326.

[11] Xu, Z.; Zhang, S.; Gao, C.; Zhao, F.; Lv, Z. S.; Feng, L. S. Chin Chem Lett 2017, 28, 159.

[12] Xu, Z.; Song, X. F.; Hu, Y. Q.; Qiang, M.; Lv, Z. S. Eur J Med Chem 2017, 138, 66.

[13] Xu, Z.; Zhang, S.; Song, X. F.; Qiang, M.; Lv, Z. S. Bioorg Med Chem Lett 2017, 27, 3643.

[14] Jin, X. H.; Xu, Y.; Yang, X. H.; Chen, X. L.; Wu, M. H.; Guan, J. G.; Feng, L. S. Curr Top Med Chem 2018, 18. https://doi.org/10.2174/1568026618666171215102031.

[15] Xu, Z.; Song, X. F.; Qiang, M.; Lv, Z. S. J Heterocyclic Chem 2017, 54, 3735.

[16] Hu, X. L.; Gao, C.; Xu, Z.; Liu, M. L.; Feng, L. S.; Zhang, G. D. Curr Top Med Chem 2018, 18. https://doi.org/10.2174/1568026618666171215101158.

[17] Xu, Z.; Song, X. F.; Hu, Y. Q.; Qiang, M.; Lv, Z. S. J Heterocyclic Chem 2017. https://doi.org/10.1002/jhet.3024.

[18] Hu, Y. Q.; Meng, L. D.; Qiang, M.; Song, X. F. J Heterocyclic Chem 2017, 54, 3725.

[19] Hu, Y. Q.; Song, X. F.; Fan, J. J. Heterocyclic Chem. 2017. https://doi.org/10.1002/jhet.3042.

[20] Feng, L. S.; Liu, M. L.; Zhang, S.; Chai, Y.; Wang, B.; Zhang, Y. B.; Lv, K.; Guan, Y.; Guo, H. Y.; Xiao, C. L. Eur J Med Chem 2011, 46, 341.